

Journal of Biomedical Optics

SPIEDigitalLibrary.org/jbo

Photochemical internalization of bleomycin for glioma treatment

Marlon S. Mathews
Joseph W. Blickenstaff
En-Chung Shih
Genesis Zamora
Van Vo
Chung-Ho Sun
Henry Hirschberg
Steen J. Madsen

Photochemical internalization of bleomycin for glioma treatment

Marlon S. Mathews,^{a,b} Joseph W. Blickenstaff,^c En-Chung Shih,^b Genesis Zamora,^b Van Vo,^c Chung-Ho Sun,^b Henry Hirschberg,^{b,c} and Steen J. Madsen^c

^aUniversity of California, Department of Neurosurgery, Irvine, 101 The City Drive South, Orange, California 92801

^bUniversity of California, Beckman Laser Institute, Irvine, 1002 Health Sciences Road East, Irvine, California 92612

^cUniversity of Nevada, Department of Health Physics and Diagnostic Sciences, Las Vegas, 4505 Maryland Parkway, Box 453037, Las Vegas, Nevada 89154

Abstract. We study the use of photochemical internalization (PCI) for enhancing chemotherapeutic response to malignant glioma cells *in vitro*. Two models are studied: monolayers consisting of F98 rat glioma cells and human glioma spheroids established from biopsy-derived glioma cells. In both cases, the cytotoxicity of aluminum phthalocyanine disulfonate (AlPcS_{2a})-based PCI of bleomycin was compared to AlPcS_{2a}-photodynamic therapy (PDT) and chemotherapy alone. Monolayers and spheroids were incubated with AlPcS_{2a} (PDT effect), bleomycin (chemotherapy effect), or AlPcS_{2a} + bleomycin (PCI effect) and were illuminated (670 nm). Toxicity was evaluated using colony formation assays or spheroid growth kinetics. F98 cells in monolayer/spheroids were not particularly sensitive to the effects of low radiant exposure (1.5 J/cm² @ 5 mW/cm²) AlPcS_{2a}-PDT. Bleomycin was moderately toxic to F98 cells in monolayer at relatively low concentrations—incubation of F98 cells in 0.1 μg/ml for 4 h resulted in 80% survival, but less toxic in human glioma spheroids respectively. In both *in vitro* systems investigated, a significant PCI effect is seen. PCI using 1.5 J/cm² together with 0.25 μg/ml bleomycin resulted in approximately 20% and 18% survival of F98 rat glioma cells and human glioma spheroids, respectively. These results show that AlPcS_{2a}-mediated PCI can be used to enhance the efficacy of chemotherapeutic agents such as bleomycin in malignant gliomas. © 2012 Society of Photo-Optical Instrumentation Engineers (SPIE). [DOI: 10.1117/JBO.17.5.058001]

Keywords: photochemical internalization; photodynamic therapy; bleomycin; AlPcS_{2a}; brain tumor; human glioma spheroids.

Paper 11790 received Dec. 24, 2011; revised manuscript received Feb. 29, 2012; accepted for publication Mar. 1, 2012; published online May 3, 2012.

1 Introduction

Statistical review at the Central Brain Tumor Registry of the United States shows that gliomas account for 34% of all primary brain tumors and 82% of all malignant primary brain tumor cases.¹ Tumor resection is the first modality employed in the treatment of gliomas.² Employing the improved surgical techniques now available, the incidence of gross tumor resection, as seen on postoperative magnetic resonance imaging (MRI), has greatly increased.^{3,4} Nevertheless, despite additional postoperative chemotherapy and radiotherapy, the great majority of glioma patients suffer a recurrence of their tumors, particularly around the margins of the surgical resection cavity.⁵ Systemically administered chemotherapy has shown poor efficacy, and survival benefits in the majority of malignant glioma patients have been modest.⁶ Chemotherapeutics need to pass the blood brain barrier (BBB) and then enter into cells through the plasma membrane, which limits chemotherapeutic agents to mostly lipophilic or low molecular weight compounds that passively diffuse into the cell cytoplasm. In contrast, many highly effective chemotherapeutic agents are large and water soluble and therefore do not easily penetrate plasma membranes but are actively transported into cells by endocytosis.⁷ Their poor ability to escape from the resulting intracellular endosomes leads to their inactivation. Therefore, in combination with modalities leading to increased endosomal escape, the

therapeutic effect of these agents would be significantly increased.

Photochemical internalization (PCI) is a technique that improves the cytosolic delivery of macromolecules in a site-specific manner.^{8–10} The concept, shown in cartoon form in Fig. 1, is to localize a photosensitizer and a desired macromolecule such as a chemotherapeutic agent in endocytic vesicles (endosomes) of tumor cells and then excite the photosensitizer with light. The resulting photochemical reaction ruptures the endosomal membrane, releasing the endosome-bound macromolecules into the cytosol and preventing lysosomal degradation. The rapid attenuation of light in the brain in turn should lead to minimal side effects, since the effect is localized to the illuminated area.

Bleomycin (BLM), first discovered in 1966, is a water-soluble glycopeptide antibiotic with a molecular weight of 1.5 kDa. It exerts its cytotoxic effects by inducing single- and double-stranded DNA breaks similar to those caused by ionizing radiation. The effects of BLM have been shown to be increased by PCI on a number of cell types, including glioma cells.^{11–15}

The limited efficacy of chemotherapy in the treatment of gliomas is caused by many factors, but two important ones are the BBB, which prevents chemotherapeutic agents from entering the brain, and limited endosomal escape of many drugs, leading to their inactivation. We have previously shown that selective site specific opening of the BBB could be obtained in the rat brain by the PCI-mediated potentiation

Address all correspondence to: Marlon S. Mathews, 101 The City Drive South, Building 56, #400, Orange, California 92801. Tel: 7144566966; Fax: (714) 456-6966; E-mail: marlonmathews@yahoo.com.

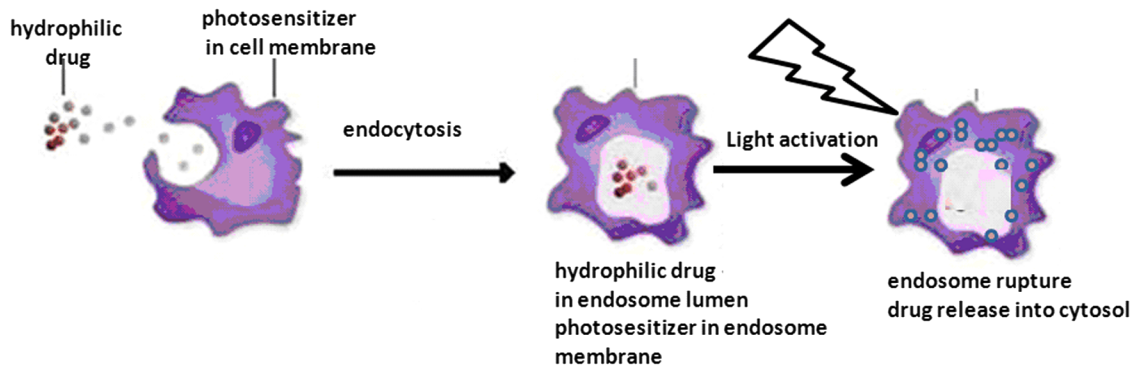


Fig. 1 Endosomal escape of hydrophilic drug by photochemical internalization. An amphiphilic photosensitizer is given before administration of the drug. The photosensitizer binds to the plasma membrane and is taken into the cell together with the drug by endocytosis. The photosensitizer and the drug co-localize in the endosomes. Since the photosensitizer is partly hydrophilic and partly hydrophobic, it will remain in the membrane of the endosome, while the hydrophilic drug will localize in the lumen. Light exposure leads to photo-induced rupture of the endosome with subsequent release of the sequestered drug into the cytosol or nucleus.

of the effects of known BBB-disrupting agents.¹⁶ BLM administered to animals with targeted BBB opening results in a significant increase in survival compared to drug-only controls. We have previously reported the results of preliminary experiments on the effects of photodynamic therapy (PDT) in combination with BLM for two different photosensitizers.^{14,15} The purpose of the study reported here was to examine in detail the other factor limiting the efficacy of BLM chemotherapy, i.e., endosomal entrapment. *In vitro* models employing rat and human glioma monolayer cultures and multicell tumor spheroids (MTS) were used to ascertain the ability of PCI to enhance the effectiveness of BLM chemotherapy.

2 Methods

2.1 Cell Lines

The F98 glioma cell line (American Type Culture Collection) used in all cell monolayer experiments was originally derived from transformed fetal CD Fisher rat brain cells following exposure to ethyl-nitrosourea on the 20th day of gestation.^{17,18} The human grade IV glioma cell line (ACBT-G. Granger, University of California, Irvine) was used in the experiments on MTS. The cells were cultured in Dulbecco's Modified Eagle Media (DMEM, Gibco, Carlsbad, CA) with high glucose and supplemented with 2 mM L-glutamine, gentamycin (100 mg/ml), and 2% heat-inactivated fetal bovine serum (Gibco). Cells were maintained at 37°C in a 7.5% CO₂ incubator.

2.2 Spheroid Generation

MTS were formed by a modification of the centrifugation method first described by Ivascu and Kubbies.¹⁹ 5×10^3 cells in 200 μ l of culture medium per well were allocated into the wells of ultra-low attachment surface 96-well round-bottomed plates (Corning Inc., NY). The plates were centrifuged at 1000 g for 10 min. Immediately following centrifugation, the tumor cells formed into a disk shape. The plates were maintained at 37°C in a 7.5% CO₂ incubator for 48 h to allow them to take on the usual three-dimensional spheroid form.

2.3 PDT Monolayer Toxicity

F98 cells were incubated in 1 μ g/ml AIPcS_{2a} (Frontier Scientific Inc., Logan, UT) and DMEM for 18 h and washed

out 4 h before illumination. Following incubation, cells were washed three times with phosphate buffered saline (PBS), and 5 ml of fresh medium was added. Irradiation was done using 670 nm light from a diode laser (Intense, North Brunswick, NJ). The cells were exposed to a range of radiant exposures (0.75 to 6 J/cm²) delivered at a light irradiance of 5 mW/cm². Following irradiation, cells were harvested with trypsin, counted using a Coulter Counter (Beckman Coulter, Model Z, Fullerton, CA) and then incubated at various cell densities in complete media for seven days to allow for colony growth. Colonies that grew from the surviving cells were stained with crystal violet and counted (>50 cells/colony) A total of four experiments were performed.

2.4 PDT Spheroid Toxicity

Forty-eight hours after generation, spheroids were transferred from the micro plate wells into 35 mm Petri dishes, 16 to 24 per dish, and incubated in 1 μ g/ml AIPcS_{2a} and DMEM for 18 h. Following incubation, spheroids were irradiated (irradiance = 5 mW/cm²; radiant exposure = 1.5 J/cm²) with 670 nm light from a diode laser. Light was coupled into a 200 μ m diameter optical fiber containing a microlens at the output end. Following irradiation, individual spheroids were placed into separate wells of a 48-well culture plate and monitored for growth. Determination of spheroid size was carried out by averaging two measured perpendicular diameters of each spheroid using a microscope with a calibrated eyepiece micrometer and their volume calculated mathematically assuming a perfect sphere. Typically, 16 to 24 spheroids were followed in each trial. Since each trial was performed three times, a total of 48 to 72 spheroids were followed for a given set of parameters. Spheroids were followed for up to 29 days.

2.5 Bleomycin Toxicity

F98 cells were incubated in varying concentrations (0.1 to 10 μ g/ml) of BLM (Sigma, St. Louis, MO) and DMEM for 4 h and then washed out. Following incubation, cells were harvested and prepared for colony assay or spheroid growth as described previously. A total of six experiments were performed.

2.6 PCI Toxicity

F98 monolayers and ACBT spheroids were incubated in 1 $\mu\text{g}/\text{ml}$ AIPcS_{2a} for 18 h followed by 4 h in various concentrations of BLM. AIPcS_{2a} was washed out 4 h before illumination. Following incubation, cells or spheroids were irradiated with 670 nm light (irradiance = 5 mW/cm²; radiant exposure = 1.5 J/cm²). Following irradiation, cells were washed, harvested, and prepared for colony growth, while individual spheroids were placed into separate wells of a 48-well culture plate and monitored for growth as described previously.

2.7 Two Photon Microscopy

Forty-eight hours after PDT or PCI treatment, the spheroids were stained using a combination of Hoechst 33342 and Ethidium Homodimer 1 (Invitrogen H1399, Carlsbad, CA) and were visualized using an inverted Zeiss laser-scanning microscope (LSM 410, Carl Zeiss, Jena, Germany) with an excitation wavelength of 488 nm. The Zeiss LSM 510 NLO Meta microscopy system is based on an Axiovert 200 M inverted microscope equipped with standard illumination systems for transmitted light and epifluorescence detection and a standard set of visible light lasers (an Argon laser 458/477/488/514 nm/30 mW, a Helium: Neon laser 543 nm/1 mW and a Helium: Neon laser 633 nm/5 mW) for confocal microscopy. It is equipped with a femtosecond Titanium: Sapphire laser excitation source (Chameleon-Ultra, Coherent) for multi-photon excitation with the exceptional tunability range from 690 to 1040 nm. The microscope platform is equipped with a motorized X-Y scanning stage and long-working distance and high numerical aperture objectives (10, 20, 40, and 100 \times). This system allows the differential visualization of cell nuclei using two-photon microscopy. Simultaneously detected blue and red emissions were isolated by using BP 390-465 infrared (IR) and BP 565-615 IR band pass filters, respectively. Fluorescent images were pseudo-colored blue (live) and red (dead).

2.8 Flow Cytometry

Flow cytometry was used to determine the fraction of viable, apoptotic, and necrotic cells in treated and control spheroids. The two different fluorescent labels used were Annexin V-FITC (Beckton, Dickson and Company, Franklin Lakes, NJ) to distinguish apoptotic cells and propidium iodide (PI; Sigma, St. Louis, MO) to label necrosis. Unlabeled cells were assumed to be viable. The spheroids were incubated in 15 mL tubes for 20 min in 500 μL of a one-to-one mixture of 1% collagenase (Invitrogen Corp., Carlsbad, CA) in Hanks' Balanced Salt Solution 1 \times (HBSS with Ca²⁺ and Mg²⁺, Invitrogen Corp., Carlsbad, CA) to dispase (Beckton, Dickson and Company, Franklin Lakes, NJ). After incubation, the spheroids were vortexed for 5 sec, and 5 mL of PBS was added. The tubes were then centrifuged in a Beckman GS-6 centrifuge (Beckman Coulter Inc., Fullerton, CA) for 5 min at 1000 rpm. The PBS was then decanted, 5 mL of PBS was added, and the tubes were vortexed for 5 sec. The tubes were centrifuged again, the PBS was decanted, and 500 μL of PBS was added. For a final time, the tubes were centrifuged, the PBS was decanted, and 1 \times binding buffer (Beckton, Dickson and Company, Franklin Lakes, NJ) was added to achieve a final concentration of 10⁶ cells/mL. Next,

100 μL of the solution was transferred along with 400 μL of 1 \times binding buffer to a 5 mL BD Falcon tube. The two labels were then added with 5 μL of Annexin V-FITC and 10 μL of 100 $\mu\text{g}/\text{mL}$ concentration PI. The solutions were gently agitated and then incubated for 15 min at room temperature in the dark. For each experiment, a set of control solutions was also prepared. One control remained unlabeled, the next labeled only with Annexin V-FITC, and the third labeled only with PI. Finally, after 15 min of incubating in the dark, each tube was analyzed in a Beckton Dickson FACSCalibur (Beckton, Dickson and Company, Franklin Lakes, NJ) flow cytometer along with CellQuest software.

2.9 Statistical Analysis

All data were analyzed and graphed using Microsoft Excel. The arithmetic mean and standard deviation were used throughout to calculate averages and errors. Statistical significances were calculated using the student's t-test, as well as the Welch's t-test. Two values were considered distinct when their p-values were below 0.05.

Synergism was calculated when analyzing PCI treatments. The equation shown below was used to determine if the PCI effect was synergistic, antagonistic, or additive, where α is the ratio of the cumulative effect of two therapies administered independently to the net effect of combining the two therapies at a given dose.

$$\alpha = \frac{SF^a \times SF^b}{SF^{ab}}$$

In this equation, SFⁱ represents the survival fraction for a specific treatment. If two treatments are to be compared, the survival fractions of each separate treatment are multiplied together and then divided by the survival fraction when both treatments were applied together. The interaction is calculated based on the dose of each treatment. The resulting number α describes the summative effect. If $\alpha > 1$, the result is synergistic (supra-additive). If $\alpha < 1$, the result is antagonistic, and if $\alpha = 1$, the result is simply additive.²⁰

3 Results

3.1 PDT and PCI on F98 Monolayers

In order to determine the optimal drug and light fluence levels for evaluating the effects of PCI on the F98 monolayers, titration of both drug and light dose were performed. The results are shown in Fig. 2(a) and 2(b) for increasing light dose and drug concentration, respectively. As expected, the data show an increase in PDT efficacy with increasing radiant exposure. The cells appeared to be sensitive to AIPcS_{2a}-PDT as indicated by the low 50% survival dose (LD₅₀). As seen in Fig. 2(b), F98 cells are also sensitive to BLM exposure. The LD₅₀ for BLM was approximately 0.5 $\mu\text{g}/\text{ml}$; nearly all cells were killed at a concentration of 10 $\mu\text{g}/\text{ml}$.

3.2 AIPcS_{2a}-PCI Efficacy on F98 Monolayers

There was a statistically significant difference in survival between cells exposed to single modality treatment (BLM or PDT) and cells subjected to PCI (Fig. 3). Greater PCI effects were observed at higher BLM concentrations. The p-values of treatment modalities compared to each other are shown in

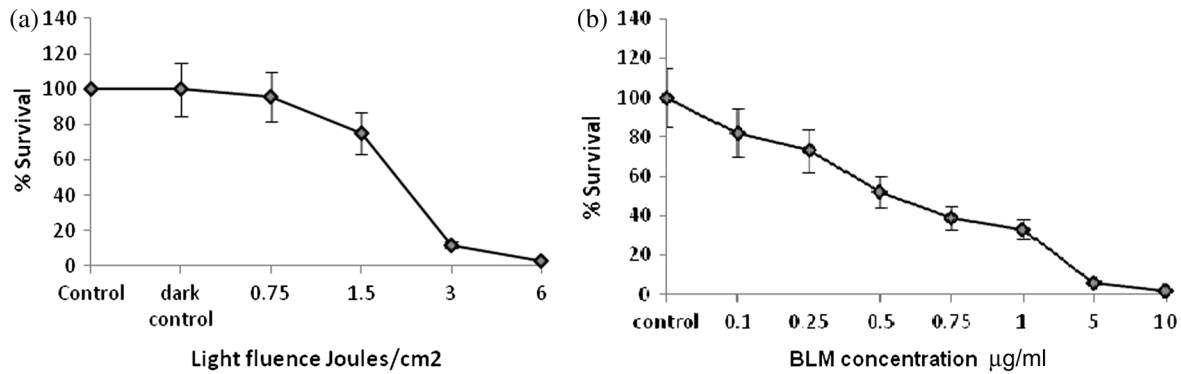


Fig. 2 (a) Effects of PDT on F98 colony formation. F98 cells incubated in 1 µg/ml AlPcS_{2a} for 18 h. Wavelength of 670 nm; light fluence 0.75 to 6 J/cm²; irradiance of 5 mW/cm². (b) Effects of 4-h incubation with increasing bleomycin (BLM) concentration (µg/ml). Each data point represents the mean of four experiments. Error bars denote standard errors.

Table 1. Since PCI is a technique which relies on the combination of drug and photosensitizer, the resultant toxicities should show more than an additive effect between BLM and AlPcS_{2a}-PDT. The degree of synergism was calculated by comparing the survival fractions of BLM and PDT alone with that of the PCI treatment for a given dose. As evidenced from the calculated α values, PCI demonstrated a synergistic effect, especially at the higher BLM concentration: $\alpha = 1.5$ and 2.7 for 0.1 and 0.25 µg/ml BLM, respectively (the higher the α value, the greater the degree of synergism).

3.3 Spheroid Growth Assays

The monolayer results clearly demonstrated a highly significant PCI effect in the F98 rat glioma cell line. The next step was to determine whether such an effect could be elicited in a more complex *in vitro* model. This was done by performing growth assays on MTS of the human glioma cell line, ACBT. Experiments were performed on four groups: (1) control, (2) AlPcS_{2a}-PDT, (3) BLM, and (4) AlPcS_{2a}-PCI (PDT+BLM) with and without light irradiation. In all experiments, 1.5 J/cm² radiant exposure and 1 µg/mL AlPcS_{2a} were used. Based on the monolayer results (Figs. 2 and 3), sub-optimal BLM and light doses, representing 70% to 80% cell survival, were chosen in order to optimize the PCI effect. Figure 4(a) shows the average growth kinetics measured over a four-week period. BLM concentrations

of 0.1 and 0.25 µg/ml were used in these experiments. Three identical experiments were performed with 16 spheroids in each group per experiment. Since the growth kinetics of the AlPcS_{2a} dark control was not significantly different from control cultures and the effects of light treatment on the BLM only (i.e., no photosensitizer) cultures were insignificant, they are omitted from the figure. As seen in the figure, both PDT and BLM induced a clear spheroid growth delay, but by week 4, the average size in these two treatment groups had reached control levels. In contrast, the average size of the PCI-treated spheroids increased only slightly during the four-week measurement interval. The α values for the PCI effects on spheroid survival at four weeks was 1.4 and 4.6 for BLM concentrations of 0.1 and 0.25 µg/ml, respectively. The toxic effects on spheroid volume growth, evaluated after four weeks in culture, of PCI of BLM were compared to the effects of BLM alone over a concentration range of 0.1 to 10 µg/ml. As can be seen from Fig. 4(b), the spheroids were much more resistant to the effects of BLM compared to cell monolayers [Fig. 2(b)]. PCI greatly enhanced the effects of the drug, and the effects of PCI with 0.1 µg/ml BLM were equivalent to those observed at 10 µg/ml of drug alone ($p < 0.05$). Figure 5 shows the average percentage (from triplicate experiments) of the spheroids that were viable four weeks following the different treatment types. Neither BLM nor AlPcS_{2a}, with or without irradiance, had a significant effect on overall spheroid survival

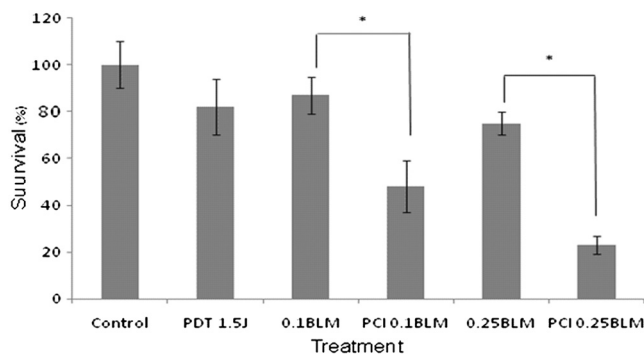


Fig. 3 Effects of BLM, PDT, and BLM PCI on F98 colony formation. F98 cells incubated in 1 µg/ml AlPcS_{2a} for 18 h. Wavelength of 670 nm; radiant exposure of 1.5 J/cm²; irradiance of 5 mW/cm² and BLM concentrations of 0.1 and 0.25 µg/ml. *designates significant differences ($p < 0.05$); each data point represents the mean of four experiments. Error bars denote standard errors.

Table 1 p -values for various F98 monolayer PCI toxicity groups. (Bleomycin concentrations 0.1 or 2.5 µg/ml; light dose 1.5 J).

Two Groups Being Compared	p -value
Control/AlPcS _{2a} (Dark)	0.9193
0.1 BLM/0.25 BLM	0.1325
1.5 J(PDT)/0.1 BLM + 1.5 J(PCI)	0.0183*
1.5 J(PDT)/0.25 BLM + 1.5 J(PCI)	0.0013*
0.1 BLM/0.1 BLM + 1.5 J(PCI)	0.0116*
0.25 BLM/0.25 BLM + 1.5 J(PCI)	0.0205*
0.1 BLM + 1.5 J(PCI)/0.25 BLM + 1.5 J(PCI)	0.0257*

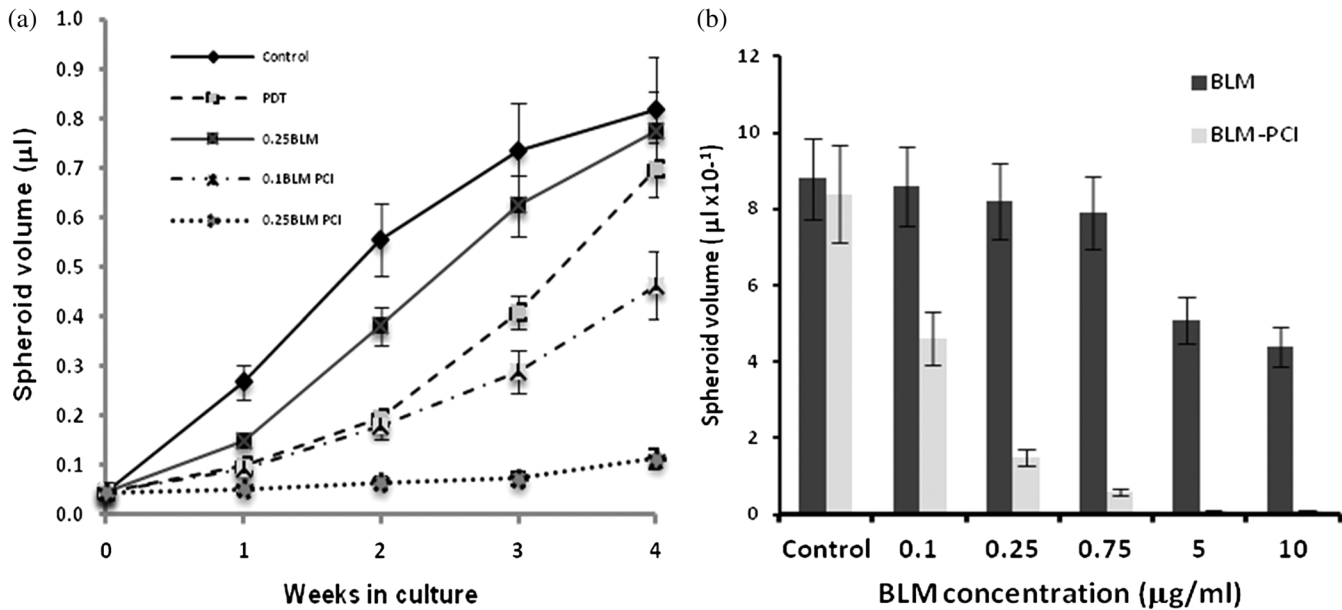


Fig. 4 Effects of BLM, PDT and BLM PCI on ACBT MTS growth. (a) Average volume growth measured in μl as a function of incubation time with 0.1 and 0.25 $\mu\text{g/ml}$ BLM. (b) Average spheroid volume measured following four weeks of incubation as a function of BLM concentration, 0.1 to 10 $\mu\text{g/ml}$. 1 $\mu\text{g/ml}$ AIPcS_{2a} incubation for 18 h. Wavelength of 670 nm; radiant exposure of 1.5 J/cm²; irradiance of 5 mW/cm². Each data point represents the mean of three experiments. Error bars denote standard errors.

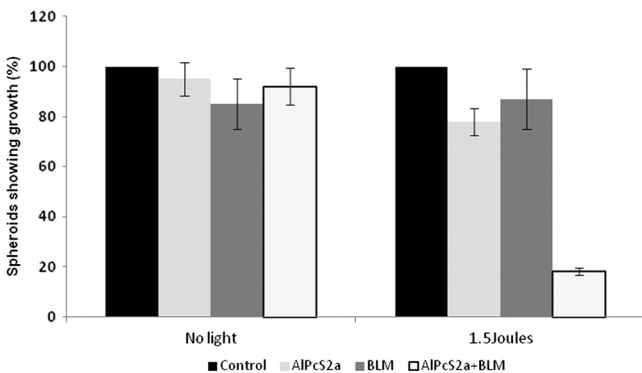


Fig. 5 Viability of control and treated ACBT MTS after four weeks in culture. 1 $\mu\text{g/ml}$ AIPcS_{2a} incubation for 18 h. Wavelength of 670 nm; radiant exposure of 1.5 J/cm²; irradiance of 5 mW/cm²; and 1-h BLM incubation at a concentration of 0.25 $\mu\text{g/ml}$. Each data point represents the mean of three experiments. Error bars denote standard errors.

after four weeks. On the other hand, there was a statistically significant ($p < 0.05$) diminution in survival of spheroids subjected to PCI (0.25 $\mu\text{g/ml}$ BLM, 1.5 J/cm² irradiation) compared to those exposed to either drug or PDT, with less than 20% of the spheroids remaining viable.

3.4 Two-Photon Fluorescence Microscopy

The results of live/dead assay employing two-photon fluorescence images demonstrated enhanced toxicity of PCI-treated spheroids compared to PDT-only treatment. This was inferred from the high proportion of red fluorescing cells observed from the PCI-treated spheroids [Fig. 6(c)]. By comparison, a smaller number of red fluorescing cells were observed from PDT-only spheroids [Fig. 6(d)], and these were mainly at the spheroid periphery. As illustrated in Fig. 6(a), virtually no dead cells were observed in control spheroids, since spheroids with a diameter of less than 400 μm do not generally have a necrotic core.

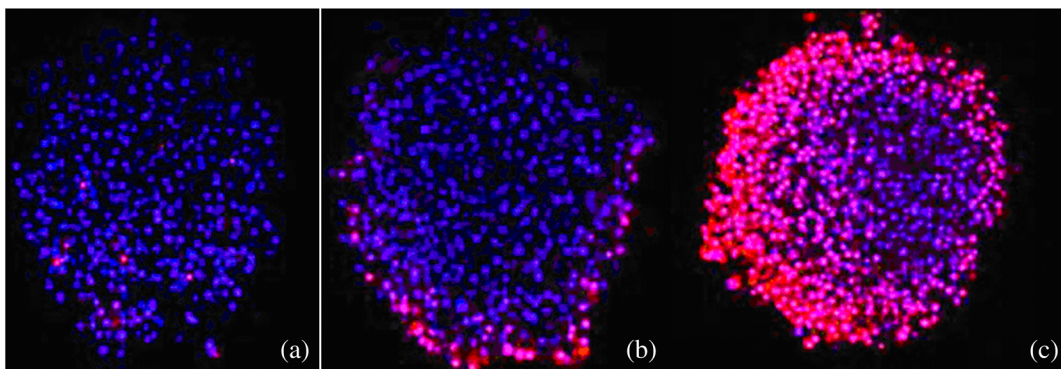


Fig. 6 Live/dead assay of control and treated spheroids. Two-photon fluorescence microscopy images of ACBT spheroids stained with Hoechst 33342 (blue: live) and Ethidium Homodimer (red: dead). Images were taken at a depth of 80 μm . Spheroids were fixed 48 h after treatment: (a) control, (b) PDT 1.5 J, (c) PCI with 0.25 $\mu\text{g/ml}$ bleomycin + 1.5 J/cm². Field of view for all images was 400 \times 400 μm .

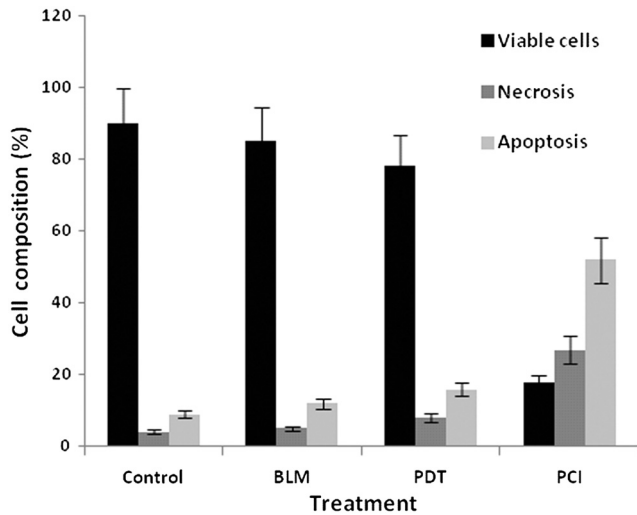


Fig. 7 Flow cytometry results. Percent composition (viable, necrotic, apoptotic) following various spheroid treatments are shown. As is evident from the figure, following PCI, cell death occurs by apoptosis as well as necrosis. However, the predominant mechanism of cell death is apoptotic.

3.5 Flow Cytometry

Determination of ACBT spheroid cell viability by flow cytometry was utilized to examine the effects of treatment on cellular viability. This was performed by examining the percentages of viable, necrotic, and apoptotic cells as a function of treatment for the control cultures and each of the three treatment groups. Forty-eight hours following BLM, PDT, or PCI treatment, the spheroids were disaggregated by collagenase treatment into a single cell suspension labeled with Annexin V-FITC to distinguish apoptotic cells and propidium iodide to label necrotic cells. The labeled cells were then passed through the cell sorter. In the PDT- and BLM-treated MTS, the majority of the cells were still viable. In sharp contrast, only 25% of the cells from the dissociated spheroids were viable following PCI treatment (Fig. 7). At the drug and light levels employed, the main mode of cell death was apoptotic.

4 Discussion

The primary objective of this study was to examine the ability of PCI to synergistically increase the efficacy of BLM chemotherapy on glioma cell monolayers and MTS. In both cases, the plasma membrane localizing photosensitizer AIPcS_{2a} was used. It was hypothesized that the combination of AIPcS_{2a}-PDT and BLM, i.e., PCI, would exhibit a synergistic toxic effect compared to either treatment modality alone. Although BLM is commonly used in a number of standard cancer therapies, including treatment of squamous cell carcinoma of the head and neck, esophagus, bronchus, skin, testis, and malignant lymphomas, it has been found to have limited use for the treatment of gliomas.¹³ Due to its hydrophilic nature and large size, it has limited penetration through the BBB. Although this is a clear disadvantage in terms of treatment efficacy, normal brain cells are protected from its toxic effects, in contrast to lipophilic chemotherapeutic agents like BCNU or TMZ now in use clinically. Thus BLM could be a highly effective drug in combination with targeted BBB opening. In a previous study, BLM was applied through a PCI-mediated targeted and localized opening of the BBB to inhibit tumor formation in a rat brain tumor

model.¹⁶ Newly implanted tumor cells were used to mimic the characteristics of infiltrating cells remaining in the resection margin usually found following surgical removal of bulk tumor. Localized BBB opening was performed 24 h after cell inoculation. This is insufficient time to allow for the development of bulk tumor and BBB degradation, but it is long enough for the cells (with a doubling time of approximately 18 h) to form small, sequestered micro-clusters, which are protected by an intact BBB. The survival of animals implanted with F98 tumor cells was significantly extended following BLM chemotherapy with PCI-mediated BBB opening compared to controls that received chemotherapy only.

Due to its hydrophilic character, BLM does not diffuse through cell plasma membranes but is actively taken up into cells by endocytosis. Its poor ability to escape from endosomes leads to inactivation by hydrolytic enzymes and complexing molecules in secondary endosomes. However, if released in the cytosol, it quickly diffuses into the nucleus, where it has a significant toxic effect.²¹ BLM has been shown to create up to 15 DNA strand breaks per molecule, making it far more efficient than any other chemotherapeutic agent. Selective electro-permeabilization, where electric pulses induce a transient and reversible permeabilization of the cell membrane, has demonstrated that as little as a few hundred internalized BLM molecules are sufficient to induce cell death.²² The cytotoxicity of BLM could be enhanced a hundred-fold by this means. These characteristics make BLM well suited for use together with PCI, where the drug is selectively released from endosomal entrapment and into the cell cytosol.

In this study, F98 cells were used as monolayer cultures to determine if the chemotherapeutic efficacy of BLM could be significantly enhanced with the application of AIPcS_{2a}-PCI. The F98 cell line's *in vitro* and *in vivo* morphology and growth have been described in detail.¹⁷ Intracranial tumors formed from this cell line have been classified as anaplastic or undifferentiated glioma with many characteristics that closely resemble those of human GBM and anaplastic astrocytoma. The data shown in Fig. 2 and Table 1 clearly indicate a significant increase in PCI-mediated BLM toxicity compared to either PDT or BLM alone at the light levels and drug concentrations used. This was not simply an additive effect of BLM together with PDT, since α values were 1.5 and 2.7 for BLM concentrations of 0.1 and 0.25 $\mu\text{g}/\text{ml}$, respectively—a clear synergistic effect.

Although the results of employing glioma cell monolayer cultures indicated a positive effect of BLM-PCI, the data obtained using this model have limitations, since these cultures are unable to mimic oxygen gradients and complex intercellular interactions found in three-dimensional tumors or tumor spheroids. In addition, the lack of an extracellular matrix in monolayer cell suspensions affects their response to a wide variety of therapies. In view of the findings that survival and cell death, especially apoptosis, depend strongly on both cell adhesion and the presence of an extracellular matrix, results obtained in monolayers are likely not a true indicator of therapeutic efficacy *in vivo*. Similar experiments to those done using cell monolayers were therefore performed using MTS, which can be considered a bridge between monolayers and animal experiments. MTS are three-dimensional aggregates of cells that mimic micro-tumors and metastases. In comparison to monolayer cultures, a significant advantage of MTS is that their micro-environment more closely mimics the *in vivo* situation,

and therefore gene expression and the biological behavior of the cells are likely similar to that encountered in tumor cells *in situ*. The oxygen gradients characteristic of MTS produce a heterogeneous population of cells that differ in their response to oxygen-dependent therapies such as ionizing radiation, PDT, and chemotherapy. In addition to oxygenation status, tumor response to these therapies is controlled by a number of parameters, including intercellular contact and communication and susceptibility to apoptosis.^{23,24} Although the light doses used in this study are relatively small, it is important to note that *in vivo* therapy will likely need higher light doses/intensity for therapeutic effect, especially for large and deeply seated tumors.²⁵ The differences in the two models explain the difference in synergistic effect (α) seen between the spheroid growth assay and monolayers at different BLM concentrations.

Treatment with BLM or PDT alone induced only a delay in MTS growth, and in general, MTS reached similar volumes as untreated controls after a few weeks in culture. However, all the MTS treated with PCI of various concentrations of BLM responded strongly to the treatment (Figs. 4 and 5). Actively growing spheroids contain proliferating cells in the periphery and nonproliferating cells in their center. The cytotoxicity induced by PDT depends on the light levels, the photosensitizer uptake, and the oxygen concentration in the different spheroid sections. In the interior of 150 μm radius spheroids, the irradiance is reduced by approximately 20%, while the oxygen concentration is reduced by around 15% compared to the periphery.^{26,27} Nevertheless, although the two-photon microscopy live/dead assays shown in Fig. 6 could demonstrate the most effective BLM PCI toxicity at the periphery, significant numbers of dead cells were also evident throughout the spheroid. However, it is important to note that, due to the limited depth of light penetration with two-photon microscopy, the superficial layers tend to generate stronger fluorescence signals. Compared to PDT, PCI appears to improve treatment of additional sub-layers of tumors than those killed by photosensitizer and light alone, because of the additional effects of the drug delivered into the cells. This has been clearly demonstrated in this study for glioma spheroids as well as in animal models for sarcomas and other types of non-central nervous system (CNS) tumors.^{12,13}

Intratumoral BLM has been attempted in the treatment of solid brain tumors in a small number of trials with very limited success.^{28,29} The rationale for the use of BLM directly into brain tumors was to avoid the problem of passage through the BBB. Electrochemotherapy with BLM on tumor-bearing rats has been done and demonstrated increased survival time compared to that of untreated animals.^{30,31} In these experiments, BLM was injected intracranially, and the effects of electroporation were very pronounced both on the tumor and on the normal brain.³¹ Although these preclinical results were encouraging, the application of electrochemotherapy to the clinical situation for the postoperative treatment of glioma patients would be extremely problematic. On the other hand, PCI-mediated drug delivery, which duplicates many of the effects of electroporation, is translatable into clinical protocols through the use of balloon catheter radiation or light applicators implanted into the resection cavity following tumor resection.^{32–34} PCI is well suited for repetitive treatment protocols, due to its localized treatment volume, reduced drug concentrations required for efficacy, and accumulation of photosensitizer in tumor tissue.

The most severe side effect of BLM is the dose-dependent induction of interstitial pneumonitis, which occurs in up to 46% of patients, with a small percent of all patients developing fatal lung fibrosis.³⁵ Some studies have indicated that the prominent lung and skin toxicity of BLM could be related to the absence of an enzyme, bleomycin hydrolase, in lung tissue. PCI of BLM significantly increases its efficacy several fold, as is clearly seen in Fig. 4(b). EC50 values determined from spheroid growth were 10 $\mu\text{l/ml}$ and 0.1 $\mu\text{g/ml}$ for BLM and PCI-BLM, respectively. Although it is difficult to translate *in vitro* results into clinical expectations, PCI has the potential to lower both drug concentrations and the number of repetitive doses required to achieve equal results to those obtained with drug alone. The toxic side effects of BLM therapy currently encountered could potentially be greatly reduced. It is important to note that it is the cumulative dose of bleomycin that correlates with the toxicity, and by a single PCI treatment, the BLM toxicity should have minor side effects. This could have significant implications for the management of patients with malignant brain tumors. More effective delivery through the BBB and increased efficacy of anti-cancer agents to infiltrating brain tumor cells remaining in the resection margin following surgery is likely to result in prolonged survival and an increased quality of life.

5 Conclusion

The results show that, with appropriately engineered delivery devices, AIPcS_{2a}-mediated PCI has the potential to enhance the efficacy of chemotherapeutic agents such as bleomycin for treatment of malignant gliomas. Further validation of the PCI effect to enhance chemotherapeutic efficacy needs to be carried out using *in vivo* models before clinical studies are to follow.

Acknowledgments

The authors are grateful for support from the Nevada Cancer Institute and the Beckman Laser Institute for institutional support. This work was supported by grants from the Norwegian Radium Hospital Foundation, Laser Microbeam and Medical Foundation (LAMMP), as well as the Chao Family Cancer Center Optical Biology Shared Resource at UCI. Disclosures: The authors report no conflicts of interest linked to the outcome of this study.

References

1. CBTRUS Statistical Report: Primary Brain Tumors in the United States 2004–2007, the Central Brain Tumor Registry of the United States (2011).
2. M. Salzman, "Epidemiology and factors affecting survival," in *Malignant Cerebral Glioma*, M. L. J. Apuzzo, Ed., pp. 95–109, American Association of Neurological Surgeons, IL (1990).
3. H. Hirschberg et al., "Impact of intraoperative MRI on the surgical results for high-grade gliomas," *J. Minimally Invasive Neurosurg.* **48**(2), 77–84 (2005).
4. W. Stummer et al., "Extent of resection and survival in glioblastoma multiforme: identification of and adjustment for bias," *Neurosurgery* **62**(3), 564–576 (2008).
5. K. E. Wallner et al., "Patterns of failure following treatment for glioblastoma multiforme and anaplastic astrocytoma," *Int. J. Radiat. Oncol. Biol. Phys.* **16**(6), 1405–1409 (1989).
6. H. Athanassiou et al., "Randomized phase II study of temozolomide and radiotherapy compared with radiotherapy alone in newly diagnosed glioblastoma multiforme," *J. Clin. Oncol.* **23**(10), 2372–2377 (2005).
7. A. Zaniboni, S. Prabhu, and R. A. Audisio, "Chemotherapy and anesthetic drugs: too little is known," *Lancet* **6**(3), 176–181 (2005).

8. K. Berg et al., "Photochemical internalization: a novel technology for delivery of macromolecules into cytosol," *Cancer Res.* **59**(6), 1180–1183 (1999).
9. K. Berg et al., "Photochemical internalization: a novel tool for drug delivery," *Curr. Pharm. Biotechnol.* **8**(6), 362–372 (2007).
10. P. K. Selbo et al., "Photochemical internalization provides time and space-controlled endolysosomal escape of therapeutic molecules," *J. Controlled Release* **148**(1), 2–12 (2010).
11. K. Berg et al., "Site-specific drug delivery by photochemical internalization enhances the antitumor effect of bleomycin," *Clin. Cancer Res.* **11**(23), 8476–8485 (2005).
12. O. J. Norum et al., "Photochemical internalization of bleomycin is superior to photodynamic therapy due to the therapeutic effect in the tumor periphery," *Photochem. Photobiol.* **85**(3), 740–749 (2009).
13. O. J. Norum, K. E. Giercksky, and K. Berg, "Photochemical internalization as an adjunct to marginal surgery in a human sarcoma model," *Photochem. Photobiol. Sci.* **8**(6), 758–762 (2009).
14. S. J. Madsen et al., "Photochemical internalization for the treatment of malignant gliomas," *Proc. SPIE* **6424**, 64242C (2007).
15. S. J. Madsen et al., "Photochemical Internalization enhances the efficacy of Bleomycin in malignant glioma cells," *Proc. SPIE* **7161**, 716132 (2009).
16. H. Hirschberg et al., "Targeted delivery of bleomycin to the brain using photo-chemical internalization of Clostridium perfringens epsilon prototoxin," *J. Neurooncol.* **95**(3), 317–329 (2009).
17. R. F. Barth, "Rat brain tumor models in experimental neurooncology: the 9L, C6, T9, F98, RG2 (D74), RT-2 and CNS-1 gliomas," *J. Neurooncol.* **36**(1), 91–102 (1998).
18. S. J. Madsen, K. Kharkhuu, and H. Hirschberg, "Utility of the F98 rat glioma model for photodynamic therapy," *J. Environ. Pathol. Toxicol. Oncol.* **26**(2), 149–155 (2007).
19. A. Ivascu and M. Kubbies, "Rapid Generation of Single-Tumor Spheroids for High-Throughput Cell Function and Toxicity Analysis," *J. Biomol. Screening* **11**(8), 922–932 (2006).
20. B. Drewinko et al., "Combination chemotherapy in vitro with adriamycin," *Cancer Biochem. Biophys.* **1**(4), 187–195 (1976).
21. B. Poddevin et al., "Very high cytotoxicity of bleomycin introduced into the cytosol of cells in culture," *Biochem. Pharmacol.* **42**(Suppl. 1), S67–75 (1991).
22. G. Pron, N. Mahrouf, and S. Orlowski, "Internalization of the bleomycin molecules responsible for bleomycin toxicity: a receptor-mediated endocytosis mechanism," *Biochem. Pharmacol.* **57**(1), 45–56 (1999).
23. P. L. Olive and R. E. Durand, "Drug and radiation resistance in spheroids: cell contact and kinetics," *Cancer Metastasis Rev.* **13**(2), 121–138 (1994).
24. M. T. Santini, G. Rainaldi, and P. L. Indovina, "Apoptosis, cell adhesion and the extracellular matrix in the three-dimensional growth of multicellular tumor spheroids," *Crit. Rev. Oncol. Hematol.* **36**(2–3), 75–87 (2000).
25. P. K. Selbo et al., "In vivo documentation of photochemical internalization, a novel approach to site specific cancer therapy," *Int. J. Cancer* **92**(5), 761–766 (2001).
26. J. Moan, K. Berg, and V. Iani, "Action spectra of dyes relevant for photodynamic therapy," in *Photodynamic Tumor Therapy*, J. G. Moser, Ed., pp. 169–181, Harwood Publishers, London (1998).
27. M. G. Nichols and T. H. Foster, "Oxygen diffusion and reaction kinetics in the photodynamic therapy of multicell tumour spheroids," *Phys. Med. Biol.* **39**(12), 2161–2181 (1994).
28. R. A. Morantz et al., "Bleomycin and brain tumors. A review," *J. Neurooncol.* **1**(3), 249–255 (1983).
29. M. Linnert and J. Gehl, "Bleomycin treatment of brain tumors: an evaluation, Anti-Cancer Drugs," Vol. **20**, pp. 157–164, Wolters Kluwer Health | Lippincott Williams & Wilkins, Philadelphia (2009).
30. L. G. Salford et al., "A new brain tumor therapy combining bleomycin with in vivo electroporation," *Biochem. Biophys. Res. Commun.* **194**(2), 938–943 (1993).
31. B. Agerholm-Larsen et al., "Preclinical Validation of Electrochemotherapy as an Effective Treatment for Brain Tumors," *Cancer Res.* **71**(11), 3753–3762 (2011).
32. T. B. Johannesen et al., "Intracavity fractionated balloon brachytherapy in glioblastoma," *Acta Neurochirurgica.* **141**(2), 127–133 (1999).
33. S. J. Madsen et al., "Development of a novel balloon applicator for optimizing light delivery in photodynamic therapy," *Lasers Surg. Med.* **29**(5), 406–412 (2001).
34. M. S. Eljamel, C. Goodman, and H. Moseley, "ALA and Photofrin fluorescence-guided resection and repetitive PDT in glioblastoma multiforme: a single centre Phase III randomised controlled trial," *Lasers Med. Sci.* **23**(4), 361–367 (2008).
35. S. Sleijfer, "Bleomycin-induced pneumonitis," *Chest* **120**(2), 617–624 (2001).